DOI: 10.1002/cbdv.202000139

FULL PAPER

CHEMISTRY & BIODIVERSITY

Synthesis, Antiproliferative and Cytotoxic Activities, DNA Binding Features and Molecular Docking Study of Novel Enamine Derivatives

Meliha Burcu Gürdere,*[a] Ali Aydin,[b] Belkız Yencilek,[a] Fatih Ertürk,[c] Oğuz Özbek,[a] Sultan Erkan,[d] Yakup Budak,[a] and Mustafa Ceylan[a]

[a] Department of Chemistry, Faculty of Arts and Sciences, Tokat Gaziosmanpaşa University, 60250 Tokat, Turkey, e-mail: burcugurdere@gmail.com

[b] Department of Basic Medical Science, Faculty of Medicine, Yozgat Bozok University, 66100 Yozgat, Turkey

[c] Vocational School, Occupational Health and Safety Program, Istanbul Arel University, 34100 Istanbul, Turkey

[d] Chemistry and Chemical Processing Technologies, Yıldızeli Vocational School, Sivas Cumhuriyet University, 58140 Sivas, Turkey

Novel enamine derivatives were synthesized from the reaction of lactone and chalcones and their antiproliferative and cytotoxic activities against six cancer cell lines (e.g., HeLa, HT29, A549, MCF7, PC3 and Hep3B) and one normal cell lines (e.g., FL) were investigated along with their mode of interactions with CT-DNA. Most of the enamine derivatives with IC_{50} values of 86–168 μM demonstrated much stronger antiproliferative activity than the starting molecules against the cancer cells. While, among the enamine derivatives, four compounds displayed higher cytotoxic potency than the control drugs (5-fluorouracil and cisplatin) against the Hep3B cell lines, these compounds did not exhibit any significant toxicity against normal cells, FL. The UV/VIS spectral data suggest that eight compounds cause hypochromism with a slight bathochromic shift (~6 nm), indicating that they bind to the DNA by way of an intercalative or minor groove binding mode. The binding constants of the compounds are in the range of $0.1\times103\ M^{-1}$–$2.3\times104\ M^{-1}$. The antiproliferative activity of studied enamine derivatives could possibly be due to their DNA binding as well as their cytotoxic properties. In addition to these assays, the chalcones and enamine derivatives were investigated by molecular docking to calculate the synergistic effect of antiproliferative activities against six human cancer cell lines.

Keywords: lactone, chalcone, enamine, antiproliferative activity, cytotoxicity, molecular docking.

Introduction

Cancer prevalence is an increasing problem for human health and life.[1] Cancer is a complex disease that varies from one patient to another in terms of manifestation, progression and outcomes. Cancer was the 7th–8th in the order of diseases leading to death at the beginning of the century; but, today it is second cause of death following cardiovascular diseases in many countries.[2] Treatment methods commonly used in cancer are surgery, radiotherapy and chemotherapy.[3] In addition to these standard treatments, hormone treatments, biological treatment methods and targeted therapies are used less frequently. It is not realistic to talk about the existence of a single definitive treatment method, because each method has its own advantages and disadvantages, and with cancer being a highly heterogeneous disease, treatment options can vary from patient to patient.[4] The development of anticancer agents with better treatment efficiency and fewer clinical side effects have attracted increased attention of the medicinal chemists as the number of cancer patients is growing rapidly.[5]

Lactones, widely found in nature, have received considerable attention because of their interesting pharmacological activities.[6] Especially, α-methylene-γ-butyrolactones have displayed anticancer

Supporting information for this article is available on the WWW under https://doi.org/10.1002/cbdv.202000139

properties.[7–10] In addition, enamines obtained from the reaction of aldehydes and ketones with secondary amines are important compounds with strong biological properties such as antibacterial,[11] anticonvulsant, anti-inflammatory,[12] and anticancer effects.[13] Moreover, natural and synthetically obtainable chalcones are among the most frequently studied compounds during the last 50 years due to their wide range of biological activities. The chalcone derivatives have been reported to have potent anticancer activity with low side effects and better solubility for therapeutic applications.[14–8] The studies mentioned above have shown us that derivatives of chalcones and lactones show excellent therapeutic effects in the treatment of many diseases, especially cancer. In addition, these derivatives have attracted the attention of researchers due to their broad antitumor spectrum, low toxicity values against non-cancer cells and immune-boosting effects. In addition, these publications have demonstrated the molecular mechanisms of antitumor potential of chalcones and lactones derivatives and have shown that these derivatives can inhibit angiogenesis, induce caspase-dependent apoptotic cell death, and regulate the expression of pro-apoptotic proteins. Therefore, it is of high importance to design and synthesize a hybrid molecule (enamine) consisting of a series of chalcones and lactones and to examine the mechanisms of action of these novel molecules on the tumor cells.

Considering the biological importance of lactones and chalcones, we have designed and synthesized a series of new hybrid molecules (enamine derivatives) by bringing the lactone and the chalcone units together with an enamine bridge. Moreover, all the synthesized compounds were evaluated for their antiproliferative activities against six human cancer cell lines (HeLa (cervical cancer), HT29 (colorectal adenocarcinoma), A549 (lung carcinoma), MCF7 (breast adenocarcinoma), PC3 (prostate adenocarcinoma), Hep3B (hepatocellular carcinoma) and against a non-cancer cell lines, FL (normal amnion epithelial cell). Among them, five compounds, **7c**, **7d**, **7e**, **7f** and **7h** displayed higher antiproliferative activity compared to the control drugs, 5-fluorouracil and cisplatin. In addition, molecular docking study was carried out to understand the binding interactions of the compounds. The binding energies between the target proteins and the studied compounds were shown to be parallel with the experimental results. We observed that the new enamine derivatives synthesized in the current study initiated apoptosis in cancer cells. Enamine derivatives may possibly lead to cancer cell death in two ways. Firstly, they may activate the apoptotic genes by directly binding to DNA. Our DNA binding experiment showed that these molecules can bind to DNA as much as control agents. Secondly, they may activate apoptotic proteins present in the cytoplasm. Molecular docking studies have shown that enamine derivatives can interact with several proteins (sirtuin 1, *Psathyrella asperospora*, epidermal growth factor receptor, and fibroblast growth factor 19) related to apoptosis and cell cycle regulation.

Results and Discussion

Chemistry

4-Aminochalcone derivatives (**3a**–**3o**) were synthesized from the Claisen–Schmidt condensation of the benzaldehyde derivatives (**1a**–**1o**) with 4-aminoacetophenone (**2**) according to the published procedure[19–22] (*Scheme 1*). In the case of 4-substituted benzaldehyde (**1k**–**1n**; methyl, methoxy, bromo and chloro), the related Schiff-base derivatives were the main products in these reactions. Due to this situation, the 4-substituted chalcone derivatives (**3k**–**3n**) were obtained by a different protocol. Firstly, the nitrochalcone derivatives (**5k**–**5n**) were synthesized by the addition of the benzaldehyde derivatives (**1k**–**1n**) to 4-nitroacetophenone (**4**). Then, the reduction of the nitro group to amino group with $SnCl_2$ gave the 4-substituted chalcone derivatives (**3k**–**3n**) (*Scheme 1*).

4-Aminochalcones (**3a**–**3o**) were reacted with lactone (**6**) in toluene in the presence of AcOH to obtain lactone-enamine derivatives (**7a**–**7o**) in the reflux conditions for 24 h. However, the yield of *p*-

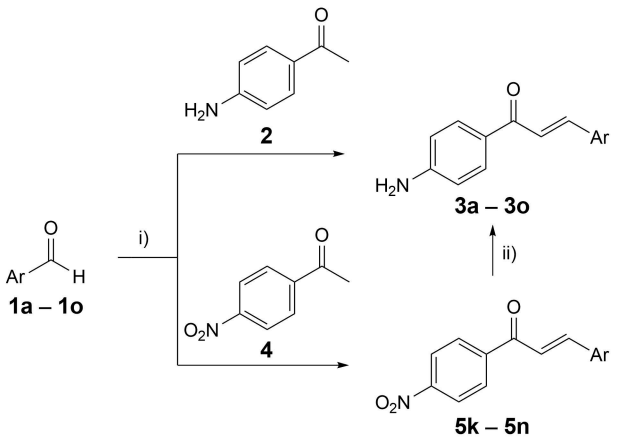

Scheme 1. Reagents and conditions: (i) NaOH, EtOH, 0 °C, 3 h, (ii) $SnCl_2{\cdot}2H_2O$, EtOH, reflux, 2 h.

substituted lactone enamines (**7k**–**7n**) was very low. For the synthesis of the enamines (**7k**–**7n**) in higher yields, the lactone enamine **8** was obtained from the reaction of 4-aminoacetophenone (**2**) with lactone (**6**), followed by the addition of *p*-substituted benzaldehydes (**1k**–**1n**) in the basic medium leading to *p*-substituted lactone enamines (**7k**–**7n**) in good yields (*Scheme 2*).

Antiproliferative Studies

Inhibition of cellular proliferation. The antiproliferative effects of the chalcones (**3a**–**3o**) and enamine derivatives (**7a**–**7o**) were assayed against human cancer cell lines; HeLa (cervical cancer), HT29 (colorectal adenocarcinoma), A549 (lung carcinoma), MCF7 (breast adenocarcinoma), PC3 (prostate adenocarcinoma), Hep3B (hepatocellular carcinoma) and a non-cancer cell line, FL (normal amnion epithelial cell). In these tests, cisplatin and 5-fluorouracil (5-FU) were used as reference anticancer drugs. IC_{50} values were calculated via Excel software with the use of absorbance data in treated and control cells and the results were given in *Table 1*.

According to IC_{50} values, all chalcone derivatives (**3a**–**3o**) showed higher activity than 5-FU against all cell lines. Compounds **3e**, **3i** and **3o** exhibited lower activity compared to cisplatin, the others displayed higher activity than cisplatin against HeLa cell lines. Compounds **3d**, **3g**, **3h**, **3j**, **3m** and **3n** demonstrated higher activity, the others showed lower activity than cisplatin against HT29 cell lines. While compounds **3a** and **3i** showed almost the same activity with cisplatin, the other compounds exhibited higher activity relative to cisplatin against A549 cell lines. All compounds (**3a**–**3o**) showed higher activity compared to cisplatin against MCF7 cell lines. Compounds **3e**–**3g**, **3l** and **3m** displayed higher activity, the others demonstrated lower activity than cisplatin against PC3 cell lines. Except compounds **3i**, **3j** and **3o**, all the other compounds exhibited higher activity than cisplatin against Hep3B cell lines. The addition of compound **3d** resulted in higher activity compared to reference chemotherapeutic agents (cisplatin and 5-FU) against all the cell lines. Among the most active chalcone derivatives (**3a**–**3o**) towards HeLa, HT29, A549, MCF7, PC3 and Hep3B cells were compounds **3b** (IC_{50} = 110.36 μM), **3g** (IC_{50} = 94.91 μM), **3m** (IC_{50} = 49.24 μM), **3d** (IC_{50} = 67.15 μM), **3m** (IC_{50} = 72.79 μM) and **3m** (IC_{50} = 59.21 μM), respectively.

Among the enamine derivatives (**7a**–**7o**), while compounds **7k** and **7l** showed lower activity than 5-FU against HeLa cell lines, all the other compounds exhibited higher activity than 5-FU against all cell lines. Except compounds **7b** and **7k**–**7n**, the other compounds displayed higher activity compared to cisplatin against HeLa cell lines. Except compounds **7a**, **7b** and **7k**–**7n**, all the other compounds displayed higher activity than cisplatin against HT29 cell lines. Except compounds **7b** and **7j**–**7n**, all the other compounds displayed higher activity compared to cisplatin against A549 cell lines. Except compounds **7b**, **7h** and **7k**–**7m**, all the other compounds demonstrated higher activity relative to cisplatin against MCF7 cell lines. While the

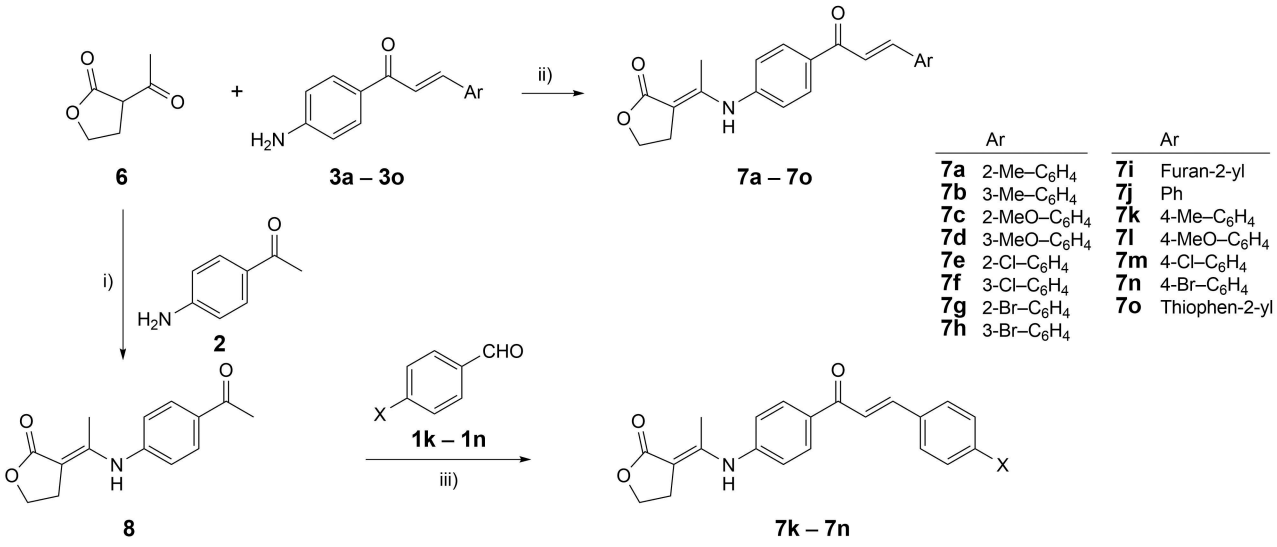

Scheme 2. Reagents and conditions: (i) toluene, AcOH, reflux, 24 h, (ii) toluene, AcOH, reflux, 24 h, (iii) NaOH, EtOH, r.t., 3 h.

Table 1. IC_{50} (μM) values of the novel compounds containing lactone, chalcone and enamine in a single structure in human cell lines.

Compound	HeLa	HT29	A549	MCF7	PC3	Hep3B	FL
3a	135.65	183.27	217.57	165.23	146.81	146.31	130.21
3b	110.36	147.07	155.54	91.31	121.15	114.03	74.50
3c	138.41	168.21	180.73	114.72	136.83	141.41	107.85
3d	114.48	120.76	100.15	67.15	100.31	63.52	64.35
3e	192.54	152.72	189.39	98.32	106.28	97.20	98.98
3f	149.58	173.33	143.57	121.26	109.61	101.43	101.89
3g	157.79	94.91	133.33	152.13	126.68	147.40	66.78
3h	138.43	101.53	126.71	173.51	151.17	143.62	77.60
3i	204.23	201.89	208.46	177.17	226.56	200.86	144.91
3j	154.38	133.60	156.67	156.76	150.84	177.76	111.03
3k	120.73	168.94	150.44	91.52	116.81	151.49	61.65
3l	117.88	142.00	129.84	71.69	101.65	119.06	60.95
3m	132.00	126.57	49.24	78.77	72.79	59.21	44.58
3n	155.07	124.89	109.57	167.88	134.26	134.12	27.83
3o	194.02	160.00	143.78	186.30	178.41	171.69	110.33
7a	118.21	326.55	142.94	91.33	100.28	56.61	95.47
7b	558.56	383.32	332.14	432.91	412.48	101.98	259.63
7c	107.78	135.02	113.04	94.46	95.37	60.95	107.37
7d	80.54	102.03	113.23	93.55	69.92	60.23	86.45
7e	109.15	114.56	129.97	100.50	74.46	45.29	112.79
7f	119.13	110.37	124.63	102.67	76.59	45.11	103.40
7g	104.20	116.78	101.96	87.10	92.84	44.31	82.78
7h	120.79	112.37	99.47	401.81	109.63	56.07	111.91
7i	127.29	124.26	376.62	100.08	136.01	147.52	102.30
7j	114.86	107.07	455.90	106.07	121.79	131.82	93.41
7k	570.93	446.43	484.24	108.51	318.93	123.05	421.63
7l	516.16	408.49	481.10	473.59	436.99	93.69	407.36
7m	542.88	404.45	382.07	417.06	327.05	76.25	307.75
7n	462.79	382.87	311.31	408.87	317.35	50.37	102.11
7o	126.60	112.81	100.64	80.81	93.13	98.14	74.74
Cisplatin	169.99	136.66	203.32	213.32	109.99	163.32	176.66
5-FU	476.62	507.38	538.13	576.56	530.44	484.31	461.25

compounds **7c**–**7i** and **7o** resulted in higher activity than cisplatin against PC3 cell lines, the activity of other compounds was lower relative to cisplatin. All compounds exhibited higher activity than cisplatin against Hep3B cell lines. Addition of the compounds **7c**–**7g** led to higher activity compared to standards (cisplatin and 5-FU) against all cell lines. Among the enamine derivatives (**7a**–**7o**), the most active compounds towards HeLa, HT29, A549, MCF7, PC3 and Hep3B cells were determined as **7d** (IC_{50} = 80.54 μM), 7d (IC_{50} = 102.03 μM), **7h** (IC_{50} = 99.47 μM), **7o** (IC_{50} = 80.81 μM), **7d** (IC_{50} = 69.92 μM) and **7g** (IC_{50} = 44.31 μM), respectively.

When the chalcones (**3a**–**3o**) and the enamine derivatives (**7a**–**7o**) were compared, the chalcone derivatives **3b** and **3k**–**3n** showed higher activity than the enamine derivatives (**7b** and **7k**–**7n**) against all cancer cell lines except Hep3B. All enamine derivatives (**7a**–**7o**) except **7m** exhibited higher activity than their corresponding chalcones (**3a**–**3o**) against Hep3B cell lines. Moreover, compounds **7a**, **7c**–**7j** and **7o** displayed higher activity than the corresponding chalcone derivatives against the HeLa cancer cell lines. While the chalones **3a** and **3g**, **3h** showed higher activity than enamines **7a** and **7g**, **7h** against HT29 cell lines, the enamines **7c**–**7e**, **7i**, **7j** and **7o** showed higher activity than chalcones **3c**–**3e**, **3i**, **3j** and **3o**. In addition, the enamines **7a**, **7c**, **7e**–**7h** and **7o** were more active than the chalcones **3a**, **3c**, **3e**–**3h** and **3o** against A549 cancer cell lines. However, the enamines **7a**, **7c**, **7f**–**7g**, **7i**, **7j** and **7o** had more activity than the chalcones **3a**, **3c**, **3f**–**3g**, **3i**, **3j** and **3o** against MCF7 cancer cell lines. The enamines except **7b** and **7k**–**7n** exhibited considerably higher activity compared to chalcones against PC3 cancer cell lines. Generally, most of the enamines (except **7a**, **7k**–**7n**) displayed

higher activity than the chalcones against especially HeLa, PC3 and Hep3B cancer cell lines. The results significantly highlight that the enamine derivatives (**7a**–**7o**) may possibly act as selective antiproliferative agents for cancer treatment, especially against HeLa, PC3 and Hep3B cancer cell lines.

Furthermore, normal cells (FL cell lines) were more sensitive to chalcone derivatives (**3a**–**3o**) (IC_{50} = ~20–100 μM) with exceptions of the **7a**, **7i**, **7j** and **7o**, compared to the cancer cells. These results point to the fact that enamine derivatives (**7a**–**7o**) may possibly act as selective antiproliferative agents which can be evaluated for their use in the treatment of cancer.

Antiproliferative activity of enamine derivatives (**7a**–**7o**) was similar between normal FL cells and cancer cells (*Table 1*). However, FL cells may have possibly lower mitochondrial activities than cancer cells and the MTT assay measures only mitochondrial activity of live cells. It is based on the principle that FL cells have decreased mitochondrial activity and are possibly exposed to increased antiproliferative effect. LDH (lactate dehydrogenase) based cytotoxicity assays were also used in addition to MTT Assay to overcome these limitations.

Cytotoxic Activity of the Compounds

The cytoplasmic lactate dehydrogenase (LDH) released to the medium from damaged plasma membranes is a marker of an increased cytotoxicity. Thus, cytotoxicity can be indirectly estimated by measuring the amount of lactate dehydrogenase in the medium with Roche's cytotoxicity detection kit. The cytotoxic activities of the enamine derivatives (**7a**–**7o**) and the chalcones (**3a**–**3o**) were evaluated after the overnight treatment of cells with the IC_{50} concentrations of the compounds. Compounds **7b** and **7k**–**7m** exhibited over 50% cytotoxicity against normal FL cells, while all other compounds **3a**–**3o** and **7a**–**7o** showed cytotoxicity in the range of 4% to 38% (*Table 2*). Some of the enamine derivatives (**7a**, **7c**–**7j** and **7o**) in the LDH

Table 2. % Cytotoxicity of the novel compounds at IC_{50} concentrations.

Compound	HeLa	HT29	A549	MCF7	PC3	Hep3B	FL
3a	28	29	32	23	42	13	15
3b	25	20	31	10	28	12	15
3c	32	34	25	22	38	10	18
3d	37	33	28	12	26	8	29
3e	43	25	32	19	22	11	7
3f	34	35	25	32	24	9	4
3g	37	28	22	62	14	38	15
3h	34	25	33	>50	38	34	5
3i	39	39	35	20	40	29	25
3j	30	41	27	17	29	36	24
3k	27	24	32	9	29	17	28
3l	41	32	34	11	25	7	34
3m	31	30	18	12	10	9	25
3n	45	36	34	27	32	29	10
3o	43	26	29	25	35	33	11
7a	20	>50	27	28	33	20	25
7b	>50	>50	>50	>50	>50	9	>50
7c	36	50	40	38	35	8	31
7d	33	27	22	32	33	7	32
7e	45	26	25	25	26	6	36
7f	42	20	20	40	32	4	34
7g	39	47	23	23	25	6	25
7h	50	34	11	>50	39	4	38
7i	42	34	>50	32	39	20	25
7j	41	43	>50	40	33	18	28
7k	>50	>50	>50	34	>50	8	>50
7l	>50	>50	>50	>50	>50	10	>50
7m	>50	>50	>50	>50	>50	4	>50
7n	>50	>50	>50	>50	>50	7	30
7o	39	29	34	20	21	15	18

assay were shown to have strong antiproliferative effects on cancer cells (IC_{50} ~44.31–147.52 μM), especially in PC3 and Hep3B cells, and were non-toxic to normal FL cells.

Comparison of MTT and LDH assays demonstrated that **7c** exhibited higher optimal antiproliferative and cytotoxic effects in comparison with both its structural isomer **3c** and the others against cancer and normal cells (*Tables 1* and *2*). The fact that **7c** is a significantly potent antiproliferative compound with IC_{50} values of 107.78, 135.02, 113.04, 94.46, 95.37, and 60.95 μM towards the growth of HeLa, HT29, A549, MCF7, PC3, and Hep3B cells, respectively, implies that **7c** may be selected as a candidate for further preclinical trials. *Tables 1* and *2* also indicate that the compounds **7d** and **7e** (IC_{50} = 80.54, 109.15 μM, respectively), the compounds **7a** and **7i** (IC_{50} = 91.33, 100.08 μM, respectively), and the compounds **7d** and **7h** (IC_{50} = 69.92, 109.63 μM, respectively) probably displayed strong antiproliferative effects against HeLa, MCF7 and PC3 cells, respectively, but were not cytotoxic to FL normal cells. This is an indication that **7d** and **7e**, the **7a** and **7i**, and the **7d** and **7h** were quite toxic for HeLa, MCF7 and PC3 cell lines, respectively, at IC_{50} concentration, but were safe for FL normal cells, therefore, these compounds may show promise in further preclinical studies.

Cell Morphology

The effects of enamine derivatives (**7a**–**7o**) on the HeLa, HT29 and MCF7 cells were investigated morphologically and the images of the treated cells compared to untreated control cells were analyzed. The images in *Figures 1*–3 indicate that untreated control cells displayed a normal cell morphology resembling those of fibroblasts or epithelial cells. On the other hand, the images obtained via phase contrast microscopy demonstrate that these compounds caused cell detachment from the surface of the flask in a dose dependent manner (*Figures 1*–3). Moreover, HeLa, HT29 and MCF7 cells exposed to enamine derivatives (**7a**–**7o**) displayed some certain morphological changes at middle and high concentrations (25–50 μg/mL) including cell shrinkage, cytoplasmic blebs and spikes, formation of abnormal globular structures and apoptotic bodies, as well as cell rounding and floating (this indicates that the cells are dead) (*Figures 1*–3). In general, concentrations of 37.5 μg/mL and above resulted in cell separation together with insufficient adhesion leading to smaller cells and decreased cell numbers.

In addition, the weak confluency, lower cell size and abnormal cellular morphology implied that reduced cell viability resulted in apoptosis. In low concentrations (< 20 μg/mL), majority of the treated cells maintained their astrocyte-like or normal fibroblast-like appearance similar to the control cells. Treatment of cells with the compounds at higher concentrations (> 37.5 μg/mL) led to cell morphologies similar to those of apoptotic cells as well as cells with cellular damage observed in affected growth (*Figures 1*–3). We also observed that the images at the bottom display some crystals grown from test compounds after which they were added to the cell medium. However, the interaction between compounds and fetal bovine serum or other components in the cell medium may cause the formation of these crystals.

Spectral Analysis of the Compounds-DNA Interactions

The mode of interactions of compounds with DNA has been evaluated by using a spectrophotometric method which compares UV/VIS absorption spectra of the free compound and compound-DNA adducts. *Figures 4* and *5* depict the interaction of these compounds with CT-DNA. UV spectra of the compounds in Tris·HCl buffer at pH 7.4 were measured separately. One intensive peak was observed in the UV spectra of **3a**, **3b**, **3d**, **3i**, **3k**, **3l**, and **3o** at ca. 365 nm and the less intensive peak observed for **3e**, **3f**, **3g**, **3j**, **3m**, and **3n** at ca. 365 nm. **3c** exhibited two peaks at ca. 365 nm and 320 nm. However, **7b** and **7l** displayed fewer intensive peaks at ca. 365, 370 nm, respectively. **7k**, **7c**, **7d**, **7e**, **7f**, **7i**, **7j**, **7m**, and **7o** displayed one intensive peak at ca. 355, 370, 360, 385, 370, 385, 380, 375, and 355 nm, respectively. Interestingly, we observed two peaks for **7a**, **7g**, **7h**, and **7n** at ca. 390 and 315 nm. The spectra of the compounds were determined in the range of 50–250 μM of DNA at 50 μM concentration of the compound at physiological pH. The spectral alterations marked the formation of the compound-DNA adduct.

Adding increasing concentrations of DNA on fixed compound concentration led to a gradual increase or decrease in the absorption intensity, resulting in a typical hyperchromic or hypochromic effect, respectively (*Table 3*) (*Figures 4* and *5*). The hyperchromic effect due to the unstacking of DNA may show the formation of stable compound-DNA complex via electrostatic interaction or groove binding mode. However, hypochromic effect due to stacking interactions in the DNA helix may display the formation of

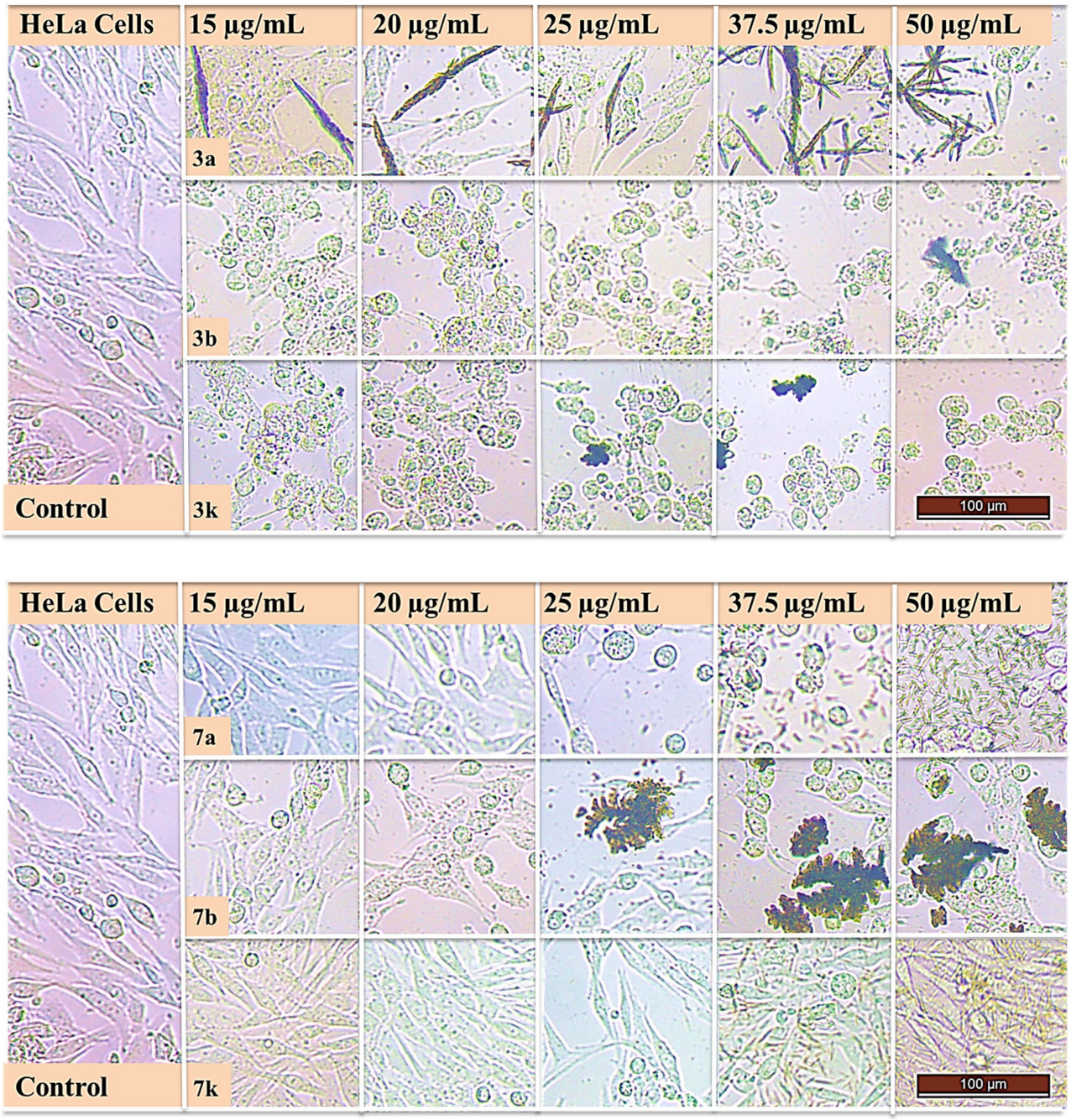

Figure 1. The analysis of cellular morphology of HeLa cells following treatments with compounds **7a**, **7b**–**7k** and **3a**, **3b**–**3k**. Morphological changes were observed under the phase-contrast microscopy following treatments at concentrations 15, 20, 25, 37.5 and 50 µg/mL of compounds **7a**, **7b**–**7k** and **3a**, **3b**–**3k** for 24 h.

compound-DNA complex via the intercalative binding mode. Thus, the absorption bands of **7c**, **7e**, **7i**, **7l**, and **7m** exhibited 23.72%, 19.0%, 41.01%, 30.0%, 23.51%, and hypochromism, respectively, with a slight bathochromic shift (~6 nm) (*Table 3*; *Figures 4* and *5*). The absorption bands of **3d**, **3i**, and **3o** also measured 13.85%, 18.86%, and 29.0% hypochromism, respectively (*Table 3*). The rest of **7a**–**7o** and **3a**–**3o** caused the hyperchromic effect in their absorption bands (*Table 3*).

The binding constant (K_b) of the compounds-DNA adduct can be determined from the alteration in absorption bands together with increasing concentrations of DNA. Benesi–Hildebrand equation, $A_0/A-A_0=$

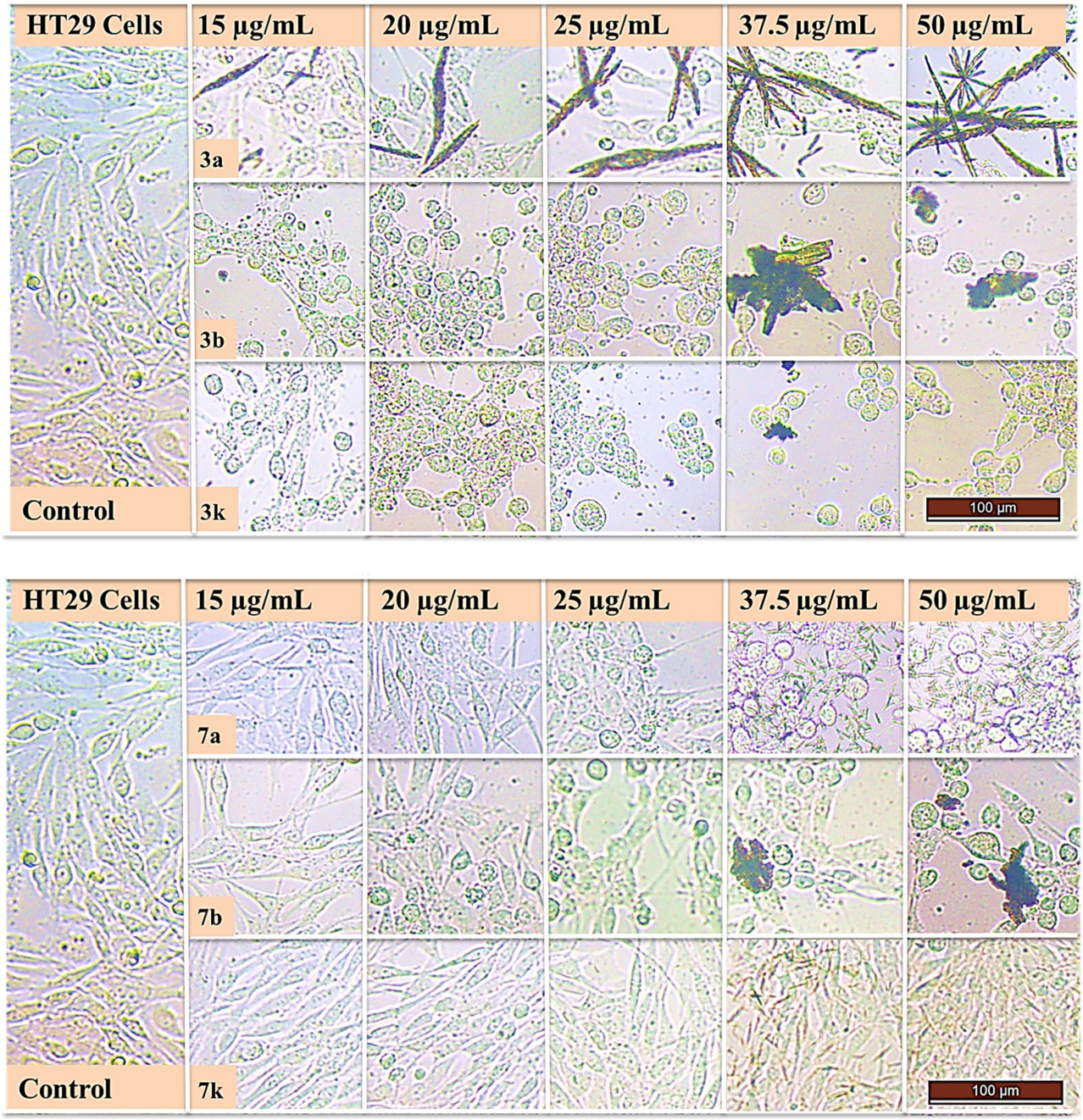

Figure 2. Analysis of cellular morphology of HT29 cells after compounds **7a**, **7b**–**7k** and **3a**, **3b**–**3k** treatments. Morphological changes were observed under the phase-contrast microscopy following treatments at concentrations 15, 20, 25, 37.5 and 50 µg/mL of compounds **7a**, **7b**–**7k** and **3a**, **3b**–**3k** for 24 h.

$\Delta_G/\Delta_{H-G}-\Delta_G+\Delta_G/\Delta_{H-G}-\Delta_G\times 1/K_b$[DNA], was used to calculate the binding constants, where K_b is the binding constant, A_0 and A represent the absorbance of each compound and its adduct with DNA and Δ_G and Δ_{H-G} denote the absorption coefficients of the compounds and the compound-DNA adducts. The binding constant can be obtained from the intercept-to-slope ratio of $A_0/(A-A_0)$ vs. 1/[DNA] plots (*Table 3*).

The K_b values of the compounds-DNA adduct are mostly consistent with the data obtained using the MTT assay. The compound **7e** depicted the strongest interactions with CT-DNA at physiological pH. Overall, the DNA binding affinity (K_b) has this order: **7e** > **3h** >

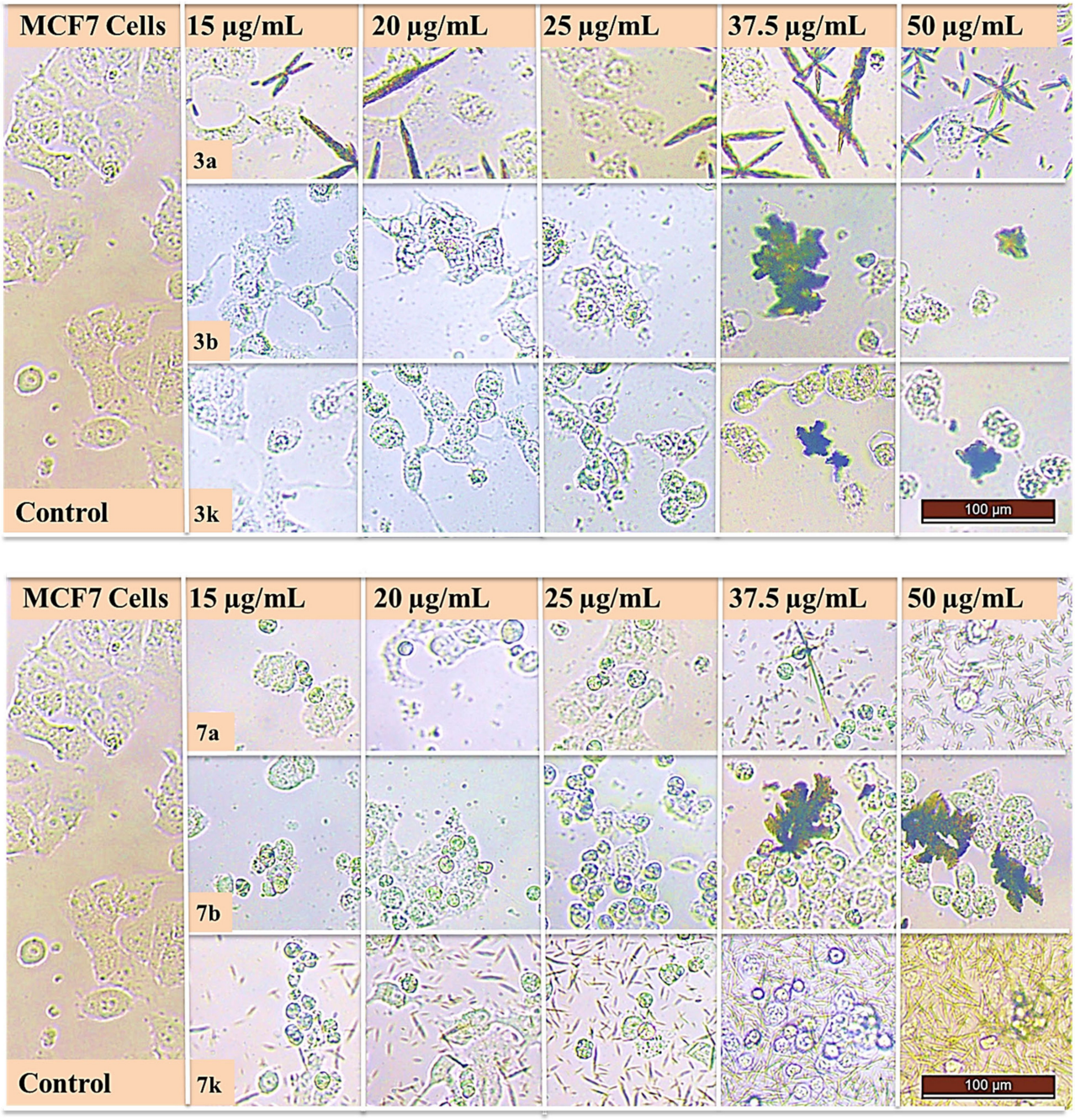

Figure 3. Analysis of cellular morphology of MCF7 cells after treatments with compounds **7a**, **7b**–**7k** and **3a**, **3b**–**3k**. Morphological changes were observed under the phase-contrast microscopy after treating cells with concentrations 15, 20, 25, 37.5 and 50 µg/mL of compounds **7a**, **7b**–**7k** and **3a**, **3b**–**3k** for 24 h.

7b > **7f** = **3f** = **3j** > **3n** > **7d** = **3m** > **7k** = **3e** > **7l** > **3k** > **7h** = **7a** > **7o** > **7n** > **3a** > **3i** > **7i** > **3o** > **7m** > **7j** > **3c** > **7c** > **3d** > **7g** > **3g** > **3b** > **3l**. Generally, the compounds **7a**–**7o** exhibited equal DNA binding activity comparable to that of **3a**–**3o**. This is an indication that antiproliferative effects of **7a**–**7o** could be estimated based on their different action mechanisms as well as their DNA binding features. K_b values of 5.73×10^4 M^{-1} and 9.7×10^4 M^{-1} of cisplatin and 5-FU, respectively, were observed to be slightly greater than those of these compounds at the same pH.[23,24]

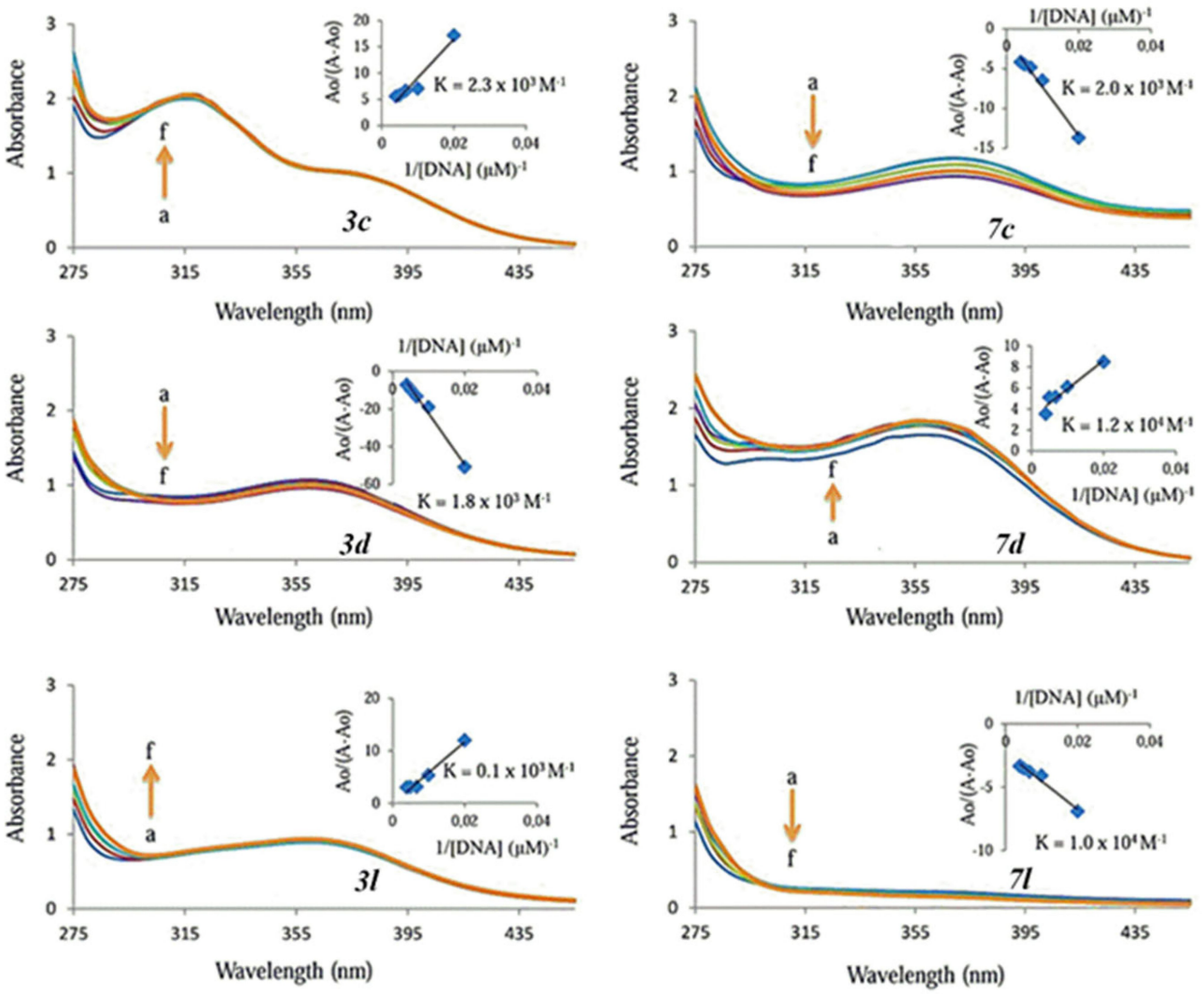

Figure 4. UV/VIS absorption spectra of 50 μM of each compound in the absence and presence of 50 μM (a), 100 μM (b), 150 μM (c), 200 μM (d) and 250 μM DNA (d). Note: The direction of arrow demonstrates the increasing concentrations of DNA. Inner graph is the plot of $A_0/(A-A_0)$ vs. 1/[DNA] to find the binding constant of the complex-DNA adduct.

Molecular Docking Analyses

The relationship between drugs and target proteins can be determined by molecular docking analyses. The target protein for HeLa (cervical cancer), HT29 (colorectal adenocarcinoma), A549 (lung carcinoma), MCF7 (breast adenocarcinoma), PC3 (prostate adenocarcinoma) and Hep3B (hepatocellular carcinoma) cell lines were chosen as the following with their PDB ID: 4I5I,[25] 5MB4,[26] 1 M17,[27] 3HY3,[28] 3 V49[29] and 5VND,[30] respectively. Sirtuin-1 is one of the histone deacetylase enzymes involved in the inactivation of p53 gene. However, the p53 gene produces a protein to kill the tumor cell. As cancer occurs, mutations in p53 gene occurs and this produces high sirtuin-1 content.[31] Human colon cancer contains *Psathyrella asperospora* with strong antiproliferative effects against HT29 cell. PAL is expressed on the cell surface of terminal *N*-acetyl-D-glucosamine (GlcNAc) found on glycoconjugates. Since terminal GlcNAc is a characteristic abnormal epitope of cancer cells, it is a very interesting antigen to be targeted for diagnosis and treatment.[32–35] A combination of PAL sequence and surface plasmon resonance (SPR) analysis is used for the amino acid sequence and three-dimensional structure of PAL. An in-depth characterization of PAL is considered using a structural basis for the specificity determined from the three-dimensional structure of the PAL/GlcNAc complex at amino acid sequence and solubility. Controlling cell life in the treatment of lung

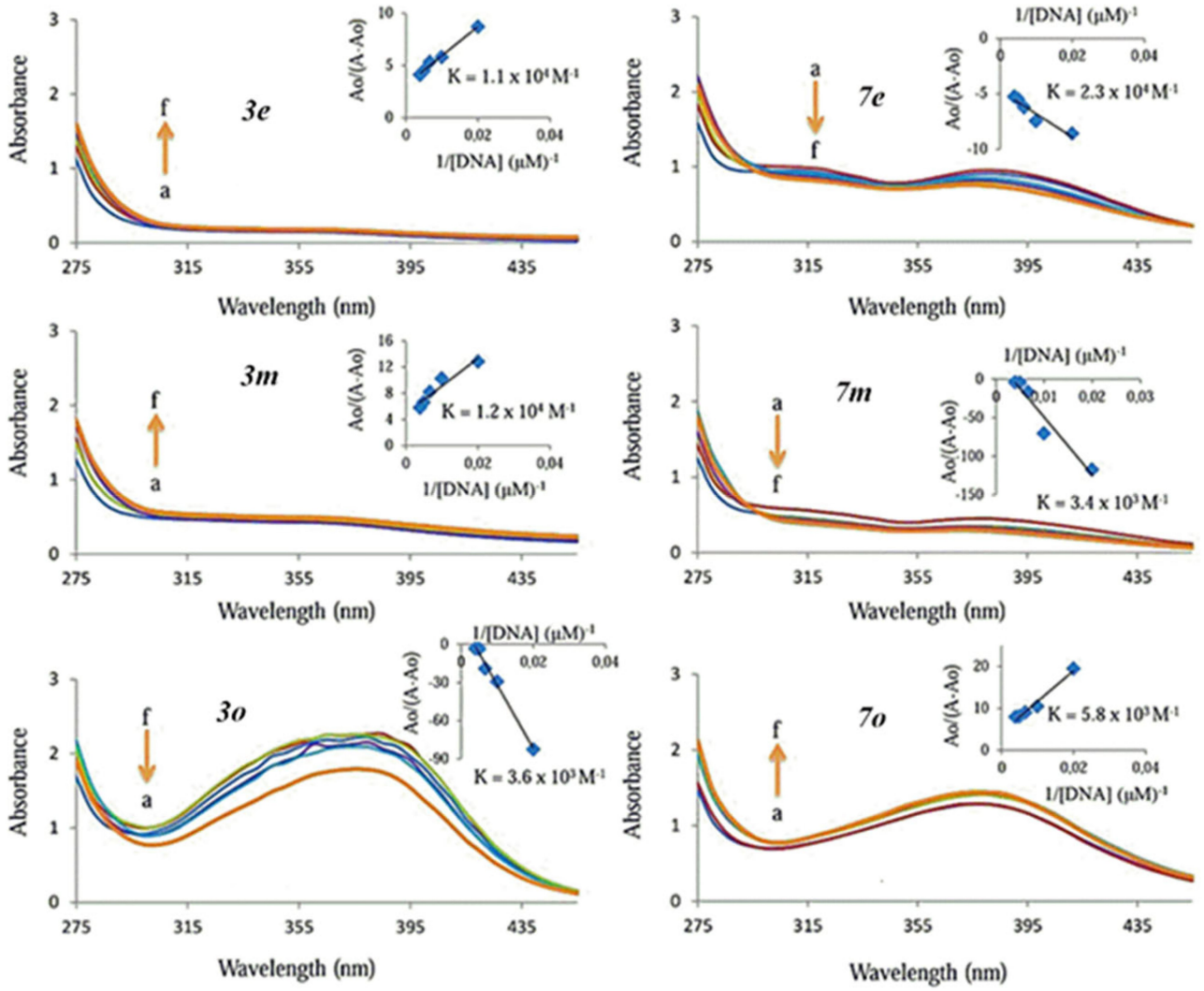

Figure 5. UV/VIS absorption spectra of 50 μM of each compound in the absence and presence of 50 μM (a), 100 μM (b), 150 μM (c), 200 μM (d) and 250 μM DNA (d). Note: The direction of arrow demonstrates increasing concentrations of DNA. Inside graph is the plot of $A_0/(A-A_0)$ vs. 1/[DNA] to find the binding constant of the complex-DNA adduct.

cancer has identified genetic and regulatory deviations that suppress cell death, promote cell division and induce tumorigenesis. One of these discoveries is the epidermal growth factor receptor (EGFR). EGFR is a transmembrane receptor tyrosine kinase protein expressed in some normal epithelial, mesenchymal and neurogenic tissues. Overexpression of EGFR has been reported in cancer and has been involved in the pathogenesis of many human malignancies, including NSCLC.[36,37] 1 M17 is the crystal structure of the epidermal growth factor receptor (EGFRK) containing forty amino acids from the carboxy terminal tail of the kinase domain.[38]

Prostate cancer (PCa) is the most commonly diagnosed cancer in men. PCa growth is mainly due to activation of the androgen receptor by androgens. PCa treatment may include surgery, hormonal therapy and the use of oral chemotherapeutic drugs. The structure based molecular insertion approach revealed the findings of (*E*)-*N*′-[(1-chloro-3,4-dihydronaphthalen-2-yl)methylene]benzohydrazide derivatives; 3 V49).[29] Hepatocellular carcinoma (HCC), which accounts for 90% of all primary liver cancers, is an important health problem.[39] Recent genomic studies of HCC have identified several oncogenic pathways, including mutations in the TERT promoter of CTNNB1, TP53 and ARID1A.[40] These studies also identify other genes, including fibroblast growth factor 19 (11q13). Three chromosomal loci containing genes containing fibroblast growth factor 19 (FGF19) and cyclin D1

Table 3. UV/VIS absorption data of compounds **7a**–**7o** and **3a**–**3o** in the absence and presence of CT-DNA.

Compound	K_b [M^{-1}]	Hypochromicity [%]	Hyperchromicity [%]
3a	4.1×10^3	–	29.16
3b	0.7×10^3	–	21.91
3c	2.3×10^3	–	17.92
3d	1.8×10^3	13.85	–
3e	1.1×10^4	–	24.46
3f	1.7×10^4	–	22.13
3g	0.8×10^3	–	35.67
3h	2.1×10^4	–	13.87
3i	4.0×10^3	18.86	–
3j	1.7×10^4	–	26.09
3k	8.3×10^3	–	22.88
3l	0.1×10^3	–	33.33
3m	1.2×10^4	–	17.31
3n	1.4×10^4	–	41.80
3o	3.6×10^3	29.00	–
7a	6.7×10^3	–	10.51
7b	1.8×10^4	–	20.12
7c	2.0×10^3	23.72	–
7d	1.2×10^4	–	28.29
7e	2.3×10^4	19.00	–
7f	1.7×10^4	–	8.63
7g	1.6×10^3	–	1.44
7h	6.7×10^3	–	16.18
7i	3.9×10^3	41.01	–
7j	3.3×10^3	–	2.61
7k	1.1×10^4	–	35.64
7 l	1.0×10^4	30.00	–
7m	3.4×10^3	23.51	–
7n	4.3×10^3	–	41.11
7o	5.8×10^3	–	12.61

(CCND1) suggest that FGF19 acts as a potential driver oncogene in HCC.[41] H3B-6527 is a highly selective and covalent small molecule inhibitor of FGFR4; and H3B-6527 monotherapy of HCC with increased FGF19 expression and H3B-6527 combination therapy with CDK4/6 inhibitor were evaluated in clinical trials for the treatment of HCC. The crystal structure of H3B-6527 attached to the ATP pocket can be found with PDB ID of 5VND.[30] The synthetic compounds and target proteins were docked with each other. The interaction energies were given in *Table 4*.

The docking results show that the binding affinities of the enamine derivatives (**7a**–**7o**) with the target proteins are higher than the binding affinities of the chalcone derivatives (**3a**–**3o**). Compounds **7c**, **7j** and **7o** exhibit interaction energy in the top row. The binding energy between 5MB4 target protein and **7j** is −336.94 kcal/mol. In addition, the other highest binding energy is between 3HY3 target protein and **3d**. The docking binding mode of these target proteins and related compounds were given in *Figure 6*. When the experimental and docking results are evaluated, it can be concluded that the studied compounds show a similar tendency towards cancer cell lines.

There are hydrogen bonds, polar and hydrophobic interactions between the **3d** drug candidate molecule and the 3HY3 target protein. H-bond forms between nitrogen atom with ILE111 and PRO112 amino acid residues. There is polar interaction between the oxygen atom and TRP109, GLN113, TYR152, THR107 and PHE85. They performed hydrophobic interaction between PRO81, TYR83, PHE85 and ILE111 with the carbon atoms of the compound **3d**. There are hydrogen bonds, pi–pi, polar and hydrophobic interactions between the **7j** drug candidate molecule and the 5MB4 target protein.

In the compound **7j**, H-bonding occurred between nitrogen atom ILE224 and ASP169 amino acids, in addition, between oxygen and THR223 amino acid.

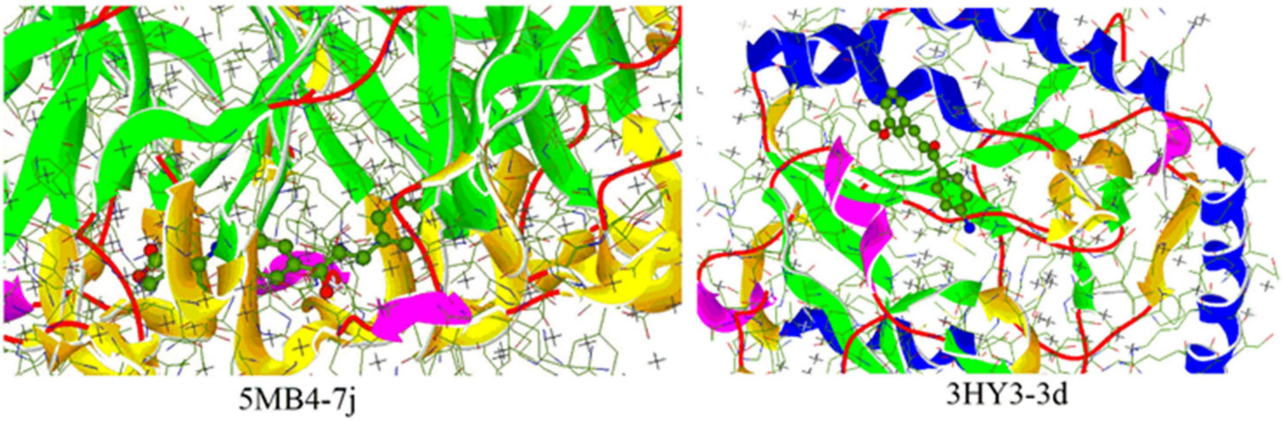

Figure 6. The docking binding mode between the target protein and compounds **7j** and **3d**.

Table 4. The interaction energies (kcal/mol) between mentioned molecules and six human cancer cell lines.

Compound	4I5I	5MB4	1M17	3HY3	3V49	5VND
3a	−246.51	−243.94	−17.92	−235.65	−250.72	−73.43
3b	−255.55	−238.25	−19.75	−276.30	−229.04	−76.61
3c	−261.63	−268.78	−16.08	−261.22	−235.08	−75.67
3d	−271.95	−250.66	−14.41	−343.97	−244.42	−78.07
3e	−242.29	239.56	−32.21	−262.26	−229.57	−71.43
3f	−265.10	−244.64	−38.23	−244.95	−244.95	−79.69
3g	−261.55	−239.02	−26.57	−267.92	−229.57	−74.79
3h	−281.84	−236.78	−31.26	−259.14	−238.75	−76.63
3i	−244.40	−333.72	−11.81	−259.36	−259.14	−238.75
3j	−255.46	−228.17	−13.71	−256.39	−227.16	−66.17
3k	−252.98	−267.11	−19.68	−263.93	−243.54	−76.81
3l	−261.29	−248.61	−21.90	−292.99	−233.45	−83.39
3m	−265.83	−245.93	−29.32	−294.12	−235.65	−88.62
3n	−257.05	−238.55	−21.90	−267.47	−227.08	−119.74
3o	−242.49	−229.05	−13.58	−239.10	−213.01	−63.31
7a	−269.48	−288.82	−20.68	−290.19	−297.25	−133.46
7b	−264.93	−312.54	−24.52	−293.12	−291.34	−122.02
7c	−325.37	−327.76	−29.16	−294.27	−295.64	−154.23
7d	−283.45	−303.18	−29.09	249.94	−284.76	−121.43
7e	−271.27	−291.83	−24.76	−279.94	−285.89	−132.28
7f	−311.26	−306.17	−25.01	−290.32	−314.73	120.24
7g	−293.98	−298.49	−16.88	−283.03	−289.88	−123.25
7h	−299.05	−313.93	−28.34	−319.85	−289.04	−134.76
7i	−266.74	−294.43	−21.03	−286.59	−271.86	−101.97
7j	−270.77	−336.94	−29.30	−289.39	−299.93	−120.44
7k	−269.83	−295.78	−26.96	−289.52	−290.23	−135.59
7l	−269.69	−301.15	−29.34	−289.12	−313.32	−125.88
7m	−271.25	−319.68	−30.86	−291.33	−292.32	−132.72
7n	−292.28	−305.64	−25.74	−294.60	−281.95	−131.53
7o	−328.64	−320.37	−29.71	−281.68	−290.09	−107.35

The number of hydrogen bonds is higher than the compound **3d**. In addition, pi–pi interaction between carbon and GLN7, polar interaction between oxygen and LEU168, ASP169 and ALA225, moreover, hydrophobic interactions with amino acid residues ALA225 and ILE224 were observed.

Conclusions

In this study, a new series of enamine derivatives (**7a**–**7o**) derived from lactone (**6**) and chalcones (**3a**–**3o**) have been successfully synthesized. The antiproliferative, cytotoxic and DNA binding properties of the compounds **7a**–**7o** and **3a**–**3o** were also investigated. Here, we focused on the certain molecules with stronger antiproliferative effects with less toxicity as well as good DNA binding properties. The studies revealed that **7c** displayed relatively optimal antiproliferative (IC_{50} = ~101.10 μM) and low cytotoxic activity (31%) similar to cisplatin and 5-FU, indicating that the compound may be a promising candidate as an antiproliferative agent. The findings point out that modification of **3c** by the substitute of lactone and chalcone results in desired molecular activation and strongly enhanced pharmacological potency. Furthermore, the interaction of **7c** with CT-DNA implied that **7c** has the optimal binding parameters with 2.0×10^3 K_b value and the hypochromism value of 23.72% of the absorption band at ca. 285 nm. Overall, this study introduced new enamine derivatives (**7a**–**7o**) as candidate lead molecules for further preclinical tests as antiproliferative agents. The binding energies between the target proteins and the compounds studied were almost in agreement with the experimental results. Considering structure–activity relationship (SAR), the compound **3b** (*m*-CH_3 which does not contain electron pair) and *p*-substituted compounds **7k**–**7n** exhibited the lowest activity against all cancer cell lines except Hep3B. The *o*- and *m*-substituted compounds **7c**–**7g** and **7o** contain thiophene ring displayed very good activity against all cancer cell

lines. Also, the compound **7a**, which contains an *o*-CH_3 substituent, and the furan-ring-containing compounds **7i** and **3i** demonstrated generally good activity. Moreover, the electron donor methoxy (OCH_3) group at the *o*- and *m*-position increased the activity.

Experimental Section

Chemistry

All chemicals and solvents were obtained from Merck (Germany) and Fluka (Germany). Melting points were measured using an Electrothermal 9100 apparatus. ^{1}H- and ^{13}C-NMR spectra were recorded with a Bruker Avance DPX-400 instrument. Elemental analyses were obtained from a LECO CHNS 932 elemental analyzer.

Synthesis of Chalcone Derivatives **3a**–**3j** *and* **5k**–**5n**

Aminochalcones **3a**–**3j** and nitrochalcone derivatives **5k**–**5n** were synthesized in accordance with published procedures.[19–22]

Reduction of **5k**–**5n** *to* **3k**–**3n**

$SnCl_2 \cdot 2H_2O$ (5 mmol) was added to a solution of **5k**–**5n** (1 mmol) in EtOH (15 mL) which was then refluxed for 2 h, after which a water solution of $NaHCO_3$ (5%, 25 mL) was added dropwise to the reaction mixture during a period of 45 min. The reaction mixture was then extracted with chloroform, the organic layer was dried over Na_2SO_4 and the solvent was removed by a rotavapor. The crude product was crystallized in a mixture of CH_2Cl_2/hexane (3:7).

General Procedure for the Synthesis of **7a**–**7o**

To a solution of chalcones **3a**–**3o** (1 mmol) in 10 mL of toluene, 3-acetyldihydrofuran-2(3*H*)-one (**6**; 1 mmol) was added and refluxed for 24 h. Then, the mixture was diluted with CH_2Cl_2 (50 mL) and dried over Na_2SO_4. The solvent was evaporated, and the crude product was crystallized in $CHCl_3$/hexane (3:7). The purity of these compounds was determined via TLC and their structures were confirmed using IR, ^{1}H-NMR, and ^{13}C-NMR.

Synthesis of **(3*E*)-3-[1-[(4-Acetylphenyl)amino]ethylidene]dihydro-2(3*H*)-furanone** (**8**)

The *p*-aminoacetophenone (**2**; 1 mmol) was dissolved in 10 mL of toluene followed by the addition of 3-acetyldihydrofuran-2(3*H*)-one (**6**; 1 mmol). After the mixture was stirred for 15 min at r.t., 2 mL of acetic acid were added and refluxed for 24 h. Then, the reaction mixture was diluted with CH_2Cl_2 (50 mL) and dried with Na_2SO_4. The solvent was removed, and the crude product was crystallized in CH_2Cl_2/hexane (3:7). The compound **8** was obtained in good yield (70%). The structure of the compound was confirmed by IR, ^{1}H- and ^{13}C-NMR (for spectral data, see *Supporting Information*).

Synthesis of **7k**–**7n**

The chalcones **7k**–**7n** were synthesized by published procedures (for spectral data, see *Supporting Information*).[19–22]

Pharmacology

Preparation of cell culture. The antiproliferative potential of the compounds was investigated on cancer cell lines, HeLa (ATCC® CCL2™), HT29 (ATCC® HTB38™), MCF7 (ATCC® HTB22™), PC3 (ATCC® CRL1435™), A549 (ATCC® CCL185™) and Hep3B (ATCC® HB8064™) and normal FL cells (ATCC® CCL62™). The cell lines were cultured in a cell medium (Dulbecco's modified Eagle's) enriched with 10% (v/v) fetal bovine serum (FBS) and 2% (v/v) penicillin-streptomycin (10,000 U/mL). First, the old medium was removed out of the flask, while the cells had reached approximately 80% confluency. Next, the cells were detached from the flask surface using 4–5 mL of trypsin-EDTA solution, and then, centrifugation was performed to remove trypsin. Afterwards, the cell pellet was suspended with 4 mL of DMEM working solution and was counted to obtain a final concentration of 5.0×10^4 cells/mL which was then inoculated into wells (100 μL cells/well).

Cell Proliferation Assay (*MTT Assay*)

A cell suspension containing approximately 1.0×10^4 cells in 100 μL was seeded into the wells of 96-well culture plates. The cells were treated overnight with the compounds and control drug, cisplatin and 5-fluorouracil (5-FU), dissolved in sterile DMSO (max. 0.5% of DMSO) at final concentrations of 2.5, 5, 10, 15, 20, 25, 37,5, and 50 μg/mL at 37 °C with 5% CO_2. The final volume of the wells was completed to 200 μL with the addition of medium.

Cell proliferation assay was evaluated using MTT (yellow tetrazolium MTT (3-(4,5-dimethylthiazol-2-yl)-

2,5-diphenyltetrazolium bromide) assay.[42] An MTT stock solution (5 mg of MTT/mL of distilled water) was filter sterilized and kept at −20 °C until further use. The cells were exposed to the MTT reagent for 4 h to form MTT formazan dye. This step was followed by the addition of dye dissolved in DMSO with Sorenson's buffer for 30 min at room temperature, after which the plate was measured at 560 nm, with 690 nm as a reference wavelength interval, using a microplate reader. Each experiment was repeated at least three times for each cell lines.

Cytotoxic Activity Assay

The cytotoxicity of the compounds, cisplatin and 5-fluorouracil on cells was determined through the use of a Lactate Dehydrogenase Assay Kit in accordance with the manufacturer's instructions.[43] Approximately 5.0×10^3 cells in 100 μL were placed in 96-well plates as triplicates and treated with IC_{50} concentrations of test compounds at 37 °C with 5% CO_2 for 24 h. LDH activity was determined using absorbance values at 492–630 nm using a microplate reader. The cytotoxicity assay results were given as the percent cytotoxicity according to the following formula: % Cytotoxicity = [(Experimental Value − Low Control/High Control − Low Control) × 100].

Cell Imaging

Cells were plated in 96-well plates at a density of 5,000 cells per well and were incubated for 24 h. Afterwards, 15, 20, 25, 37.5, and 50 μg/mL of the test compounds were administered and morphology alterations of the cells were screened by phase contrast microscopy for every 6 h during 24 h. Images of control and test compound treated cells were taken at the end of the process using a digital camera attached to an inverted microscope.

DNA Binding Studies

UV spectroscopy was used to determine the interaction of the compounds with CT-DNA and to calculate the binding constants (K_b). A CT-DNA solution was prepared by dissolving 2.5 mg CT-DNA in 10.0 mL Tris·HCl buffer (20 mM Tris·HCl, 20 mM NaCl at pH 7.4) which was then stored in the refrigerator. The concentration of CT-DNA was determined spectrophotometrically using the known ε value of 6600 M^{-1} cm^{-1} at 260 nm. After dissolving the CT-DNA fibers in Tris·HCl buffer, the purity of this solution was checked using the absorbance ratio A_{260}/A_{280}. The CT-DNA solution in the buffer displayed an A_{260}/A_{280} ratio of 1.89, indicating that the DNA was sufficiently pure. These compounds were dissolved in DMSO and diluted with Tris·HCl buffer to obtain 50 μM concentrations. Test compounds in the solutions were incubated at 37 °C for about 30 min before the measurements. The UV absorption titrations were conducted by keeping the concentration of these compounds fixed while varying the CT-DNA concentrations (50–250 μM). Absorption spectra were recorded using 1-cm-path quartz cuvettes at room temperature.

Calculation of IC_{50} and % Inhibition

The IC_{50} value is a concentration that inhibits half of the cells *in vitro*. The half maximal inhibitory concentrations (IC_{50}) of the test and control compounds were calculated using XLfit5 or an excel spreadsheet and represent μM at 95% confidence intervals. The proliferation assay results were expressed as percent inhibition according to the following formula: % Inhibition = [1 − (Absorbance of Treatments/Absorbance of DMSO) × 100].

Docking Study

Docking studies were performed by the optimization of ligands and obtaining proteins corresponding to the specific cancer cell lines from the protein database. The molecular drawings of studied ligands were prepared by using GausView 5.0.8 and the mechanic optimizations were calculated with Gaussian 09 W.[44,45] Molecular docking studies were performed between HEX 8.0.0 program for the complexes studied and the target protein.[46]

Acknowledgements

The authors are indebted to the Gaziosmanpasa University, Scientific Research Projects Commission (Project No: BAP-2015/91) and TÜBİTAK (Scientific and Technological Research Council of Turkey; Project No. 114Z696) for financial supports.

Author Contribution Statement

M. B. G., B. Y., F. E., O. Ö., Y. B. and M. C. designed and performed the experiments, analyzed the data, and M.

B. G. and M. C. wrote the article. A. A. performed the antiproliferative activity experiments, analyzed the data of compounds. S. E. carried out the molecular docking study of compounds.

References

[1] T. I. Santana, M. O. Barbosa, P. A. T. M. Gomes, A. C. N. Cruz, T. G. Silva, A. C. L. Leite, 'Synthesis, anticancer activity and mechanism of action of new thiazole derivatives', *Eur. J. Med. Chem.* **2018**, *144*, 874–886.

[2] Cancer Fact Sheet, Feb. 2017, World Health Organisation, 2017.

[3] L. Wayteck, K. Breckpot, J. Demeester, S. C. de Smedt, K. Raemdonck, 'A personalized view on cancer immunotherapy', *Cancer Lett.* **2014**, *352*, 113–125.

[4] S. K. Kandi, S. Manohar, C. E. V. Gerena, B. Zayas, S. V. Malhotra, D. S. Rawat, 'C_5-curcuminoid-4-aminoquinoline based molecular hybrids: design, synthesis and mechanistic investigation of anticancer activity', *New J. Chem.* **2015**, *39*, 224–234.

[5] K. Lal, P. Yadav, 'Recent advancements in 1,4-disubstituted 1*H*-1,2,3-triazoles as potential anticancer agents', *ACS Med. Chem.* **2018**, *18*, 21–37.

[6] D. R. Nicponski, '4-(Dimethylamino)pyridine as a catalyst for the lactonization of 4-hydroxy-2-methylenebutanoate esters', *Tetrahedron Lett.* **2014**, *55*, 2075–2077.

[7] P. V. Ramachandran, M. A. Helppi, A. L. Lehmkuhler, J. M. Marchi, C. M. Schmidt, M. T. Yip-Schneider, 'Factors influencing the cytotoxicity of α-methylene-γ-hydroxy esters against pancreatic cancer', *Bioorg. Med. Chem. Lett.* **2015**, *25*, 4270–4273.

[8] R. Shanmugam, P. Kusumanchi, H. Appaiah, L. Cheng, P. Crooks, S. Neelakantan, T. Peat, J. Klaunig, W. Matthews, H. Nakshatri, C. Sweeney, 'A water soluble parthenolide analog suppresses in vivo tumor growth of two tobacco associated cancers, lung and bladder cancer, by targeting NF-κB and generating reactive oxygen species', *Int. J. Cancer* **2011**, *128*, 2481–2494.

[9] K. Lesiak, K. Koprowska, I. Zalesna, D. Nejc, M. Duchler, M. Czyz, 'Parthenolide, a sesquiterpene lactone from the medical herb feverfew, shows anticancer activity against human melanoma cells in vitro', *Melanoma Res.* **2010**, *20*, 21–34.

[10] W. Gladkowski, A. Skrobiszewski, M. Mazur, M. Siepka, A. Pawlak, B. Obminska-Mrukowicz, A. Bia1onska, D. Poradowski, A. Drynda, M. Urbaniak, 'Synthesis and anticancer activity of novel halolactones with β-arylsubstituents from simple aromatic aldehydes', *Tetrahedron* **2013**, *69*, 10414–10423.

[11] C. Wang, G. A. Russell, 'γ-Lactone formation in the addition of benzenesulfonyl bromide to diene and enyne esters', *J. Org. Chem.* **1999**, *64*, 2066–2069.

[12] J. P. Michael, C. B. Koning, G. D. Hosken, T. V. Stanbury, 'Reformatsky reactions with *N*-arylpyrrolidine-2-thiones: synthesis of tricyclic analogs of quinolone antibacterial agents', *Tetrahedron* **2001**, *57*, 9635–9648.

[13] D. L. Boger, T. Ishizaki, J. R. J. Wysocki, S. A. Munk, P. A. Kitos, O. Suntornwat, 'Total synthesis and evaluation of (±)-*N*-(*tert*-butoxycarbonyl)-CBI, (±)-CBI-CDPI1, and (±)-CBI-CDPI2:CC-1065 functional agents incorporating the equivalent 1,2,9,9a-tetrahydrocyclopropa[1,2-*C*]benz[1,2-*e*] indol-4-one (CBI) left-hand subunit', *J. Am. Chem. Soc.* **1989**, *111*, 6461–6463.

[14] H. M. Wang, L. Zhang, J. Liu, Z. L. Yang, H. Y. Zhao, Y. Yang, D. Shen, K. Lu, Z. C. Fan, Q. W. Yao, Y. M. Zhang, Y. Teng, Y. Peng, 'Synthesis and anti-cancer activity evaluation of novel prenylated and geranylated chalcone natural products and their analogs', *Eur. J. Med. Chem.* **2015**, *92*, 439–448.

[15] S. Park, E. H. Kim, J. Kim, S. H. Kim, I. Kim, 'Biological evaluation of indolizine-chalcone hybrids as new anticancer agents', *Eur. J. Med. Chem.* **2018**, *144*, 435–443.

[16] P. Yadav, K. Lal, A. Kumar, S. K. Guru, S. Jaglan, S. Bhushan, 'Green synthesis and anticancer potential of chalcone linked 1,2,3-triazoles', *Eur. J. Med. Chem.* **2017**, *126*, 944–953.

[17] D. Coskun, M. Erkisa, E. Ulukaya, M. F. Coskun, F. Ari, 'Novel 1-(7-ethoxy-1-benzofuran-2-yl) substituted chalcone derivatives: Synthesis, characterization and anticancer activity', *Eur. J. Med. Chem.* **2017**, *136*, 212–222.

[18] Y. Wang, S. Xue, R. Li, Z. Zheng, H. Yi, Z. Li, 'Synthesis and biological evaluation of novel synthetic chalcone derivatives as anti-tumor agents targeting, Cat L and Cat K', *Bioorg. Med. Chem.* **2018**, *26*, 8–16.

[19] M. B. Gürdere, H. Gezegen, Y. Budak, M. Ceylan, 'Iodine-catalyzed addition of methyl thioglycolate to chalcones', *Phosphorus Sulfur Silicon Relat. Elem.* **2012**, *187*, 889–898.

[20] M. B. Gürdere, A. C. Emeç, O. N. Aslan, Y. Budak, M. Ceylan, 'Triethylamine-mediated addition of 2-aminoethanethiol hydrochloride to chalcones: synthesis of 3-(2-amino-ethylthio)-1-(aryl)-3-(thiophen-2-yl)propan-1-ones and 5,7-diaryl-2,3,6,7-tetrahydro-1,4-thiazepines', *Synth. Commun.* **2016**, *46*, 536–545.

[21] M. B. Gürdere, O. Özbek, M. Ceylan, 'Aluminum chloride-catalyzed C-alkylation of pyrrole and indole with chalcone and bis-chalcone derivatives', *Synth. Commun.* **2016**, *46*, 322–331.

[22] Ü. M. Kocyigit, Y. Budak, M. B. Gürdere, F. Ertürk, B. Yencilek, P. Taslimi, İ. Gülçin, M. Ceylan, 'Synthesis of chalcone-imide derivatives and investigation of their anticancer and antimicrobial activities, carbonic anhydrase and acetylcholinesterase enzymes inhibition profiles', *Arch. Physiol. Biochem.* **2018**, *124*, 61–68.

[23] T. Mosmann, 'Rapid colorimetric assay for cellular growth and survival: application to proliferation and cytotoxicity assays', *J. Immun. Meth.* **1983**, *65*, 55–63.

[24] T. Decker, M. L. Lohmann-Matthes, 'A quick and simple method for the quantitation of lactate dehydrogenase release in measurements of cellular cytotoxicity and tumor necrosis factor (TNF)activity', *J. Immun. Meth.* **1988**, *115*, 61–69.

[25] R. Dennington, T. Keith, J. Millam, 2009 Gauss View 5.0. Gaussian Inc., Wallingford.

[26] M. J. Frisch, G. W. Trucks, H. B. Schlegel, G. E. Scuseria, M. A. Robb, J. R. Cheeseman, G. Scalmani, V. Barone, B. Mennucci, G. A. Petersson, H. Nakatsuji, M. Caricato, X. Li, H. P. Hratchian, A. F. Izmaylov, J. Bloino, G. Zheng, J. L. Sonnenberg, M. Hada, M. Ehara, K. Toyota, R. Fukuda, J. Hasegawa, M. Ishida, T. Nakajima, Y. Honda, O. Kitao, H. Nakai, T.

Vreven, J. A. Montgomery Jr., J. E. Peralta, F. Ogliaro, M. Bearpark, J. J. Heyd, E. Brothers, K. N. Kudin, V. N. Staroverov, R. Kobayashi, J. Normand, K. Raghavachari, A. Rendell, J. C. Burant, S. S. Iyengar, J. Tomasi, M. Cossi, N. Rega, J. M. Millam, M. Klene, J. E. Knox, J. B. Cross, V. Bakken, C. Adamo, J. Jaramillo, R. Gomperts, R. E. Stratmann, O. Yazyev, A. J. Austin, R. Cammi, C. Pomelli, J. W. Ochterski, R. L. Martin, K. Morokuma, V. G. Zakrzewski, G. A. Voth, P. Salvador, J. J. Dannenberg, S. Dapprich, A. D. Daniels, Ö. Farkas, J. B. Foresman, J. V. Ortiz, J. Cioslowski, D. J. Fox, Gaussian 09 (Gaussian, Inc., Wallingford CT, 2009).

[27] M. A. Husain, S. U. Rehman, H. M. Ishqi, T. Sarwar, M. Tabish, 'Spectroscopic and molecular docking evidence of aspirin and diflunisal binding to DNA: a comparative study', *RSC Adv.* **2015**, *5*, 64335–64345.

[28] C. N. N'soukpoé-Kossi, C. Descôteaux, E. Asselin, H. A. G. Tajmir-Riahi, Bérubé, 'DNA interaction with novel antitumor estradiol-platinum(II) hybrid molecule: A comparative study with cisplatin drug', *DNA Cell Biol.* **2008**, *27*, 101–107.

[29] D. K. Jangir, S. Charak, R. Mehrotra, S. Kundu, 'FTIR and circular dichroism spectroscopic study of interaction of 5-fluorouracil with DNA', *J. Photochem. Photobiol. B* **2011**, *105*, 143–148.

[30] A. L. Nasyanka, 'Docking, synthesis, and cytotoxic activity of *N*-4-methoxybenzoyl-*N*′-(4-fluorophenyl) thiourea on HeLa cell lines', *Thai J. Pharm. Sci.* **2017**, *41*, 99–102.

[31] J. P. Ribeiro, M. Ali Abol Hassan, R. Rouf, E. Tiralongo, T. W. May, C. J. Day, A. Varrot, 'Biophysical characterization and structural determination of the potent cytotoxic *Psathyrella asperospora* lectin', *Proteins Struct. Funct. Bioinf.* **2017**, *85*, 969–975.

[32] S. Yakaiah, P. S. V. Kumar, P. B. Rani, K. D. Prasad, P. Aparna, 'Design, synthesis and biological evaluation of novel pyrazolo-oxothiazolidine derivatives as antiproliferative gents against human lung cancer cell line A549', *Bioorg. Med. Chem. Lett.* **2018**, *28*, 630–636.

[33] D. Wu, Y. Li, G. Song, C. Cheng, R. Zhang, A. Joachimiak, N. Shaw, Z. J. Liu, 'Structural basis for the inhibition of human 5,10-methenyltetrahydrofolate synthetase by N10-substituted folate analogs', *Cancer Res.* **2009**, *69*, 7294–7301.

[34] A. Ha, E. Ramakrishnan, R. Muthiah, A. Bhattacharjee, S. Kabilan, 'Design, synthesis, and biological evaluation of (*E*)-*N*′-((1-chloro-3,4-dihydronaphthalen-2-yl)methylene) benzohydrazide derivatives as anti-prostate cancer agents', *Front. Chem.* **2019**, *7*, 474.

[35] J. J. Joshi, H. Coffey, E. Corcoran, J. Tsai, C. L. Huang, K. Ichikawa, V. Rimkunas, 'H3B-6527 is a potent and selective inhibitor of FGFR4 in FGF19-driven hepatocellular carcinoma', *Cancer Res.* **2017**, *77*, 6999–7013.

[36] Z. Wang, Y. Sun, 'Targeting p53 for novel anticancer therapy', *Transl. Oncol.* **2010**, *3*, 1–12.

[37] R. Rouf, A. S. Stephens, L. Spaan, N. X. Arndt, C. J. Day, T. W. May, J. Tiralongo, 'G2/M cell cycle arrest by an *N*-acetyl-D-glucosamine specific lectin from *Psathyrella asperospora*', *Glycoconj. J.* **2014**, *31*, 61–70.

[38] A. Audfray, M. Beldjoudi, A. Breiman, A. Hurbin, I. Boos, C. Unverzagt, J. Le Pendu, 'A recombinant fungal lectin for labeling truncated glycans on human cancer cells', *PLoS One* **2015**, *10*, e0128190.

[39] J. P. Singh, K. Zhang, J. Wu, X. Yang, '*O*-GlcNAc signaling in cancer metabolism and epigenetics', *Cancer Lett.* **2015**, *356*, 244–250.

[40] O. Machon, S. F. Baldini, J. P. Ribeiro, A. Steenackers, A. Varrot, T. Lefebvre, A. Imberty, 'Recombinant fungal lectin as a new tool to investigate *O*-GlcNAcylation processes', *Glycobiology* **2017**, *27*, 123–128.

[41] K. Inamura, H. Ninomiya, Y. Ishikawa, O. Matsubara, 'Is the epidermal growth factor receptor status in lung cancers reflected in clinicopathologic features', *Arch. Pathol. Lab. Med.* **2010**, *134*, 66–72.

[42] Y. Ohsaki, S. Tanno, Y. Fujita, E. Toyoshima, S. Fujiuchi, Y. Nishigaki, K. Kikuchi, 'Epidermal growth factor receptor expression correlates with poor prognosis in non-small cell lung cancer patients with p53 overexpression', *Oncol. Rep.* **2000**, *7*, 603–610.

[43] J. Stamos, M. X. Sliwkowski, C. Eigenbrot, 'Structure of the epidermal growth factor receptor kinase domain alone and in complex with a 4-anilinoquinazoline inhibitor', *J. Biol. Chem.* **2002**, *277*, 46265–46272.

[44] S. Torrecilla, J. M. Llovet, 'New molecular therapies for hepatocellular carcinoma', *Clin. Res. Hepatol. Gastroenterol.* **2015**, *39*, S80–S85.

[45] J. Zucman-Rossi, A. Villanueva, J. C. Nault, J. M. Llovet, 'Genetic landscape and biomarkers of hepatocellular carcinoma', *Gastroenterology* **2015**, *149*, 1226–1239.

[46] R. Pinyol, J. C. Nault, I. M. Quetglas, J. Zucman-Rossi, J. M. Llovet, 'Molecular profiling of liver tumors: classification and clinical translation for decision making', *Semin. Liver Dis.* **2014**, *34*, 363–375.

Received February 28, 2020
Accepted May 5, 2020

